

# Molecular Dynamics Studies of the Buffalo Prion Protein Structured Region at Higher Temperatures

Jiapu Zhang

Centre of Informatics and Applied Optimisation, Federation University Australia, Mount Helen Campus, Ballarat, Victoria 3353, Australia;

Tel: +61-3-5327 6335; Emails: j.zhang@federation.edu.au, jiapu\_zhang@hotmail.com

**Abstract:** Molecular dynamics (MD) studies of buffalo prion protein (BufPrP<sup>C</sup>) [Zhang et al. (2016) J Biomol Struct Dyn 34(4):762–777] showed that the structure of this protein is very stable at room temperature (whether under neutral pH or low pH environments). In order to understand the reason why buffalo is resistant to prion diseases and why BufPrP<sup>C</sup> is so stable at room temperature, this paper will prolong our MD running time at room temperature and extend our research to higher temperatures to study this BufPrP<sup>C</sup> structure furthermore. From the salt bridge point of view we found an important reason why BufPrP<sup>C</sup> is so stable at room temperature; this might be a nice clue of drug discovery or drug design for the treatment of prion diseases. In conclusion, this brief article talks about the MD results of BufPrP at different temperatures, and presents a clue to seek the reasons of the conversion from normal cellular prion protein (PrP<sup>C</sup>) to diseased infectious prions (PrP<sup>Sc</sup>). This should be very useful for the goals of medicinal chemistry in prion diseases research fields.

**Key words:** buffalo PrP; stable protein structure; room temperature; higher temperatures; drug discovery or design.

## Introduction

Unlike bacteria and viruses, which are based on DNA and RNA, prions are unique as disease-causing agents since they are misfolded proteins. Prions propagate by deforming harmless, correctly folded proteins into copies of themselves. The misfolding is irreversible. Prions attack the nervous system of the organism, causing an incurable, fatal deterioration of the brain and nervous system until death occurs. Some examples of these diseases are mad cow disease in cattle, chronic wasting disease in deer and elk, and Creutzfeldt-Jakob disease in humans.

Not every species is affected by prion diseases. Water buffalo is a species being resistant to prion diseases. The research question arises: from the molecular structure point of view, what is the reason that allows it to retain its molecular structure folding? This is the research question addressed in this paper. Many experimental studies have shown that BufPrP is very stable so that it resists to the infection of diseased prions [Iannuzzi et al., 1998; Oztabak et al., 2009; Imran et al., 2012; Zhao, et al., 2012; Uchida et al., 2014; Qing et al., 2014, Zhao et al., 2017; Yaman et al., 2017 & 2018] - the brief review of these experimental studies can be seen in [Zhang et al., 2016]. In addition, in 2015 Zhao et al. (2015) reported that the prion protein gene polymorphisms associated with

bovine spongiform encephalopathy susceptibility differ significantly between cattle and buffalo [Zhao et al., 2015] and reported three significant findings in buffalo: 1) extraordinarily low deletion allele frequencies of the 23- and 12-bp indel polymorphisms; 2) significantly low allelic frequencies of six octarepeats in coding sequence; and 3) the presence of S4R, A16V, P54S, G108S, V123M, S154N and F257L substitutions in buffalo coding sequences [Zhao et al., 2015]. In 2017, Zhao et al. (2017) reported that fixed differences in the 3'UTR of buffalo PRNP gene provide binding sites for miRNAs post-transcriptional regulation [Zhao et al., 2017]. In 2017, Yaman et al. (2017) Investigated the prion protein gene (PRNP) polymorphisms in Anatolian, Murrah, and crossbred water buffaloes (*Bubalus bubalis*) and in 2018, Yaman et al. (2018) reported the T/A and T/G genotypes in water buffaloes for the first time; they found: 1) three synonymous single nucleotide polymorphisms (SNP) at positions 126, 234, and 285, and a non-synonymous SNP at position 322 (G108S) were detected; 2) triplet G/A/T base substitutions were observed at position 126 and two additional genotypes, T/A and T/G, at this position were determined; and 3) six octarepeats that indicated the presence of the wild-type PRNP6 allele in the coding region [Yaman et al., 2018].

As we all know, prion diseases are caused by the conversion from normal cellular prion protein ( $\text{PrP}^C$ ) to diseased infectious prions ( $\text{PrP}^{Sc}$ ); in structure the conversion is mainly from  $\alpha$ -helices to  $\beta$ -sheets (generally  $\text{PrP}^C$  has 42%  $\alpha$ -helix and 3%  $\beta$ -sheet, but  $\text{PrP}^{Sc}$  has 30%  $\alpha$ -helix and 43%  $\beta$ -sheet [Griffith, 1967; Jones et al., 2005; Daude, 2004; Ogayar et al., 1998; Pan et al., 1993; Reilly, 2000]). The structural region of a  $\text{PrP}^C$  usually consists of  $\beta$ -strand 1 ( $\beta 1$ ),  $\alpha$ -helix 1 (H1),  $\beta$ -strand 2 ( $\beta 2$ ),  $\alpha$ -helix 2 (H2),  $\alpha$ -helix 3 (H3), and the loops linked them each other]. The conformational changes may be amenable to study by molecular dynamics (MD) techniques. NMR experiences showed that a prion resistant species does not have higher conformational stability at higher temperature than nonresistant species [Yu et al., 2016]; this means at high temperature the  $\alpha$ -helices of  $\text{PrP}^C$  will turn to  $\beta$ -sheets of  $\text{PrP}^{Sc}$  so that we can find out some secrets of the protein structural conformational changes of PrP. Hence, in this paper we will use MD to study the molecular structure of buffalo prion protein  $\text{BufPrP}^C(124-227)$  [Zhang et al., 2016]. In [Zhang et al., 2016], the structure of  $\text{BufPrP}^C(124-227)$  is showed very stable at room temperature, whether under neutral pH or low pH environments. In order to understand the reason why buffalo is resistant to prion diseases and why  $\text{BufPrP}^C$  is so stable at room temperature, this paper will prolong our MD running time at room temperature and extend our research to higher temperatures to study this  $\text{BufPrP}^C$  structure furthermore - the Methods and Materials section will be briefly given in the next section. In the section of Results and Discussion, we will analyze our MD computational results and discuss a reason why  $\text{BufPrP}^C$  is so stable at room temperature. The Conclusions section presents a concluding remark of this paper and propose a nice clue from  $\text{BufPrP}$  studies for drug discovery/design of the treatment of prion diseases.

## Materials and Methods

The MD structure used for the paper is the one of [Zhang et al., 2016], i.e. the structured region BufPrP structure. In [Zhang et al., 2016], 25 ns' MD simulations were done for room temperature 300 K. This paper prolongs the MD running time to 30 ns. Moreover, this paper extends 30 ns' MD simulations to higher temperatures 350 K and 450 K respectively. The MD methods for 350 K [Zhang, 2012] and 450 K [Zhang, 2010; Zhang, 2011; Zhang et al., 2011; Zhang et al., 2015] are completely same as the ones of [Zhang, 2010; Zhang, 2011; Zhang, 2012; Zhang et al., 2011; Zhang, 2015; Zhang et al., 2015]. We emphasize that all of our methods are completely reproducible [Chen et al., 2016].

BufPrP has stable molecular structures at 300 K during the whole 25 ns' MD simulations [Zhang et al., 2016], where the root mean square deviation (RMSD) and Radius Of Gyration values are not changing very much during the whole 25 ns. As we all know, RMSD and Radius Of Gyration are two indicators for structural changes in a protein. The Radius Of Gyration is the mass weighted scalar length of each atom from the center-of-mass (COM). The RMSD is used to measure the scalar distance between atoms of the same type for two structures. In this paper, the initial structures compared with all the MD structures are the minimized/optimized structures. From the RMSD and Radius Of Gyration observations for 300 K, 350 K and 450 K, we then carry out deeper researches on the secondary structures developments during the whole 30 ns' MD simulations of 300 K, 350 K, 450 K. The BufPrP molecular structure is maintained by a network of atoms by their peptide bonds, covalent bonds (e.g. the disulfide bond S-S between Cys179 and Cys214), and noncovalent bonds such as hydrogen bonds, salt links, van der Waals contacts, and hydrophobic interactions. We will find out which bonds are contributing to maintain the stability of BufPrP.

## Results and Discussion

We first present the RMSD (Figure 1) and Radius Of Gyration (Figure 2) results of BufPrP at 300 K, 350 K and 450 K respectively during the whole 30 ns.

In Figures 1–2 [Zhang, 2018], we see that (i) at 300 K and 350 K, the values of RMSD and Radius Of Gyration are not changing very much (RMSDs varying within 2 angstroms and Radius Of Gyration varying within 1 angstrom - these are within normal variations of MD structures because typically we would want our RMSD to be less than 1.5–2 angstroms), whether under neutral or low pH environments; (ii) the RMSD performance of (i) happens at 450 K under neutral pH environment but RMSDs varying largely nearly within 7 angstroms (however from Figure 3 we think the  $\alpha$ -helices are still unfolded under neutral pH environment at 450 K because variations of Radius Of Gyration are normally within 2 angstroms), and the Radius Of Gyration performance of 450 K under neutral pH environment is slight worse than at 300 K and 350 K but still normally varying within 2 angstroms; and (iii) at 450 K under low pH environment, for seed2, it is clear that the  $\alpha$ -helices are unfolded into  $\beta$ -structures. Thus, next we just see the Secondary Structure graphs of BufPrP at 450 K, low pH value (Figure 3).

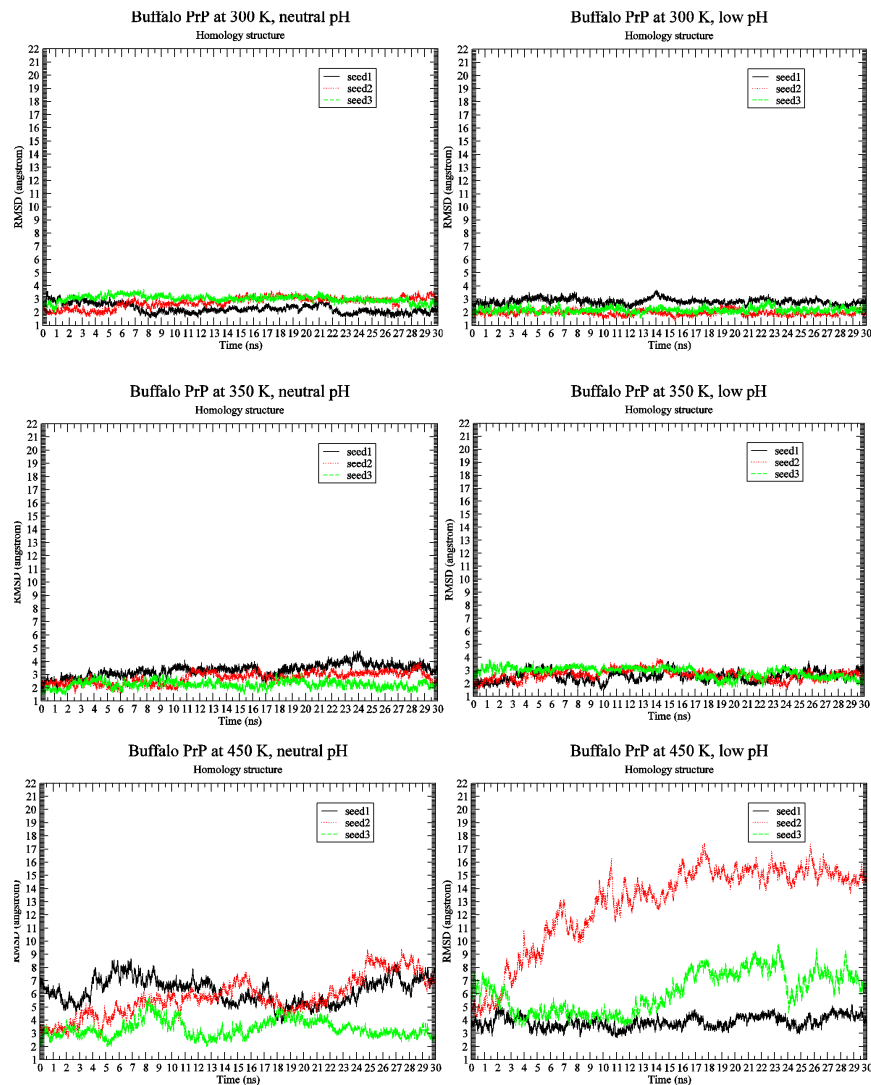


Figure 1: RMSD of BufPrP at 300 K, 350 K and 450 K, neutral and low pH values (up to down: 300 K, 350 K, 450 K; left: neutral pH, right: low pH) during 30 ns' MD.

Seeing Figure 3, we know that not only for seed2 but also for seed3,  $\alpha$ -helices H1 and H2 unfold into other forms of secondary structures. In summary, in the below we may only focus on low pH environment at 450 K to find out reasons of the unfolding of  $\alpha$ -helices H1 and H2.

Because the change of pH environments from neutral pH to low pH will make the loss of salt bridges, we will mainly analyze the noncovalent bonds of salt bridges (SBs) as follows (Tables 1–2).

We can see in Tables 1–2 the following SBs with high occupied rates at 300 K, 350 K and 450 K during the whole 30 ns of MD simulations:

- SBs in H1:

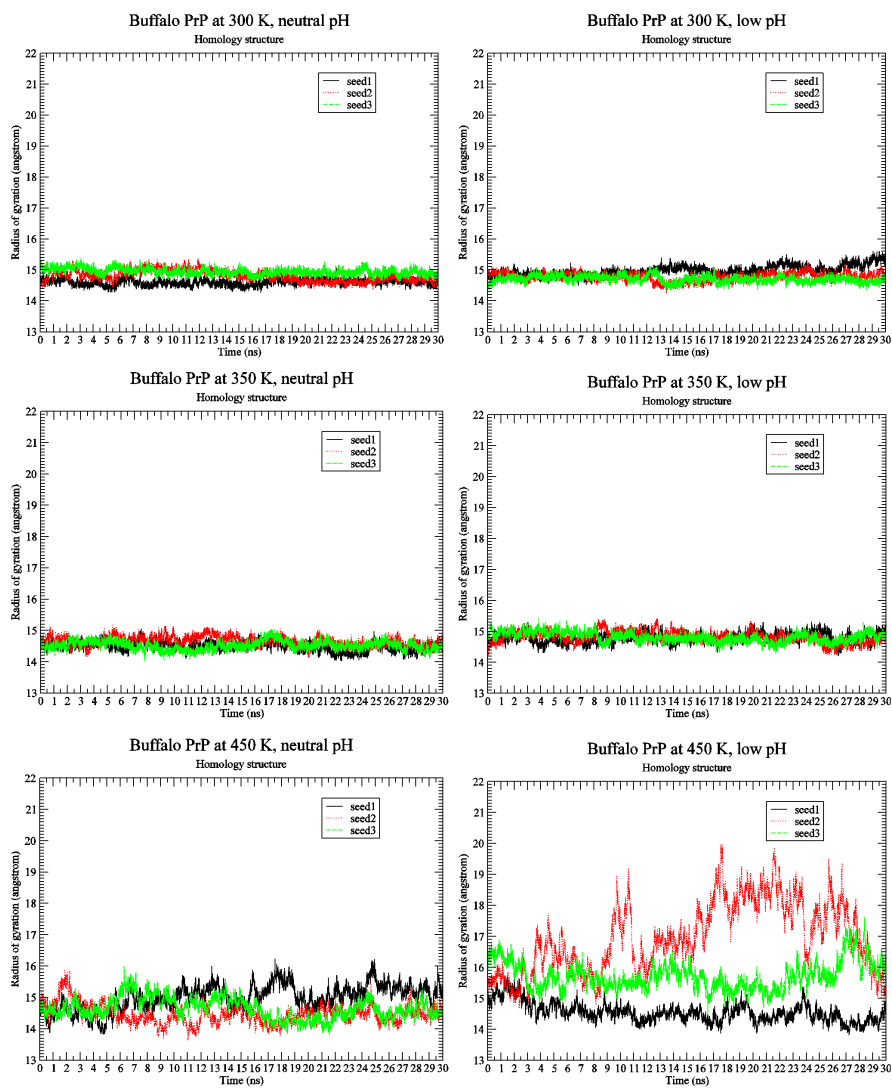


Figure 2: Radius Of Gyration of BufPrP at 300 K, 350 K and 450 K, neutral and low pH values (up to down: 300 K, 350 K, 450 K; left: neutral pH, right: low pH) during 30 ns' MD.

- ASP147-ARG148,
- HIS155-ARG156,
- GLU152-ARG148,
- GLU152-ARG151,
- ASP147-ARG151,
- ASP147-HIS140,
- SBs in H2:
  - GLU186-LYS185,

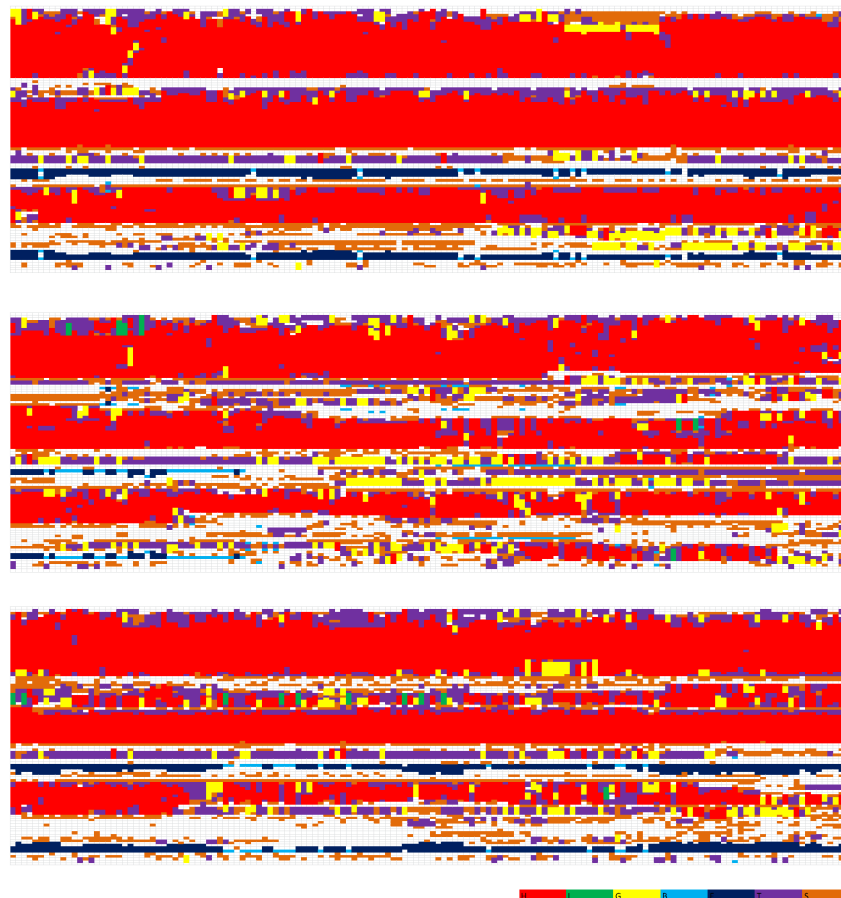


Figure 3: Secondary Structure graphs of BufPrP at 450 K, low pH value (up to down: seed1–seed3; X-axis: time (0–30 ns), Y-axis: residue number (124–227); H is the  $\alpha$ -helix, I is the 5 helix or called  $\pi$ -helix, G is the 3-helix or called  $3_{10}$  helix, B is the residue in isolated  $\beta$ -bridge, E is the extended strand (participates in  $\beta$ -ladder), T is the hydrogen bonded turn, and S is the bend) during 30 ns' MD.

- HIS187–LYS185,
- ASP178–HIS177,
- SBs in H3:
  - GLU211–ARG208,
  - GLU207–LYS204,
  - GLU221–ARG220,
  - GLU207–ARG208,
- special SBs:
  - ASP178–ARG164 - linking the  $\beta$ 2- $\alpha$ 2 loop,

Table 1: Percentages (%) of some salt bridges (between two residues) under neutral pH environment for BufPrP at 300 K, 350 K and 450 K during 30 ns' MD:

Buffalo PrP/ Salt Bridges (SBs)	300 K			350 K			450 K		
	seed1	seed2	seed3	seed1	seed2	seed3	seed1	seed2	seed3
ASP147@CG-ARG148@CA.CZ	100	100	100	100	100	100	99.95	99.97	99.98
HIS155@CG-ARG156@CA.CZ	99.74	99.80	99.63	99.80	99.87	99.75	99.72	99.40	99.50
HIS155@NE2-ARG156@CA.CZ	5.18	6.53	7.49	31.90	46.75	13.26	24.63	18.23	22.53
GLU211@CD-ARG208@CA.CZ	99.47	99.70	93.46	91.26	98.07	99.67	97.08	97.38	95.88
GLU207@CD-LYS204@CA.NZ	98.48	99.88	99.86	99.19	98.05	98.63	87.38	97.52	97.67
GLU221@CD-ARG220@CA.CZ	96.78	63.88	52.51	96.77	87.26	94.58	69.02	69.40	77.25
GLU186@CD-LYS185@CA.NZ	93.63	92.88	96.30	68.63	84.71	86.76	19.93	77.72	74.98
ASP178@CG-ARG164@CA.CZ	87.89	23.89	1.51	38.56	33.93	47.25	4.30	30.45	39.87
GLU196@CD-LYS194@CA.NZ	70.57	60.08	19.20	28.13	20.43	5.61	4.65	26.40	25.12
GLU207@CD-ARG208@CA.CZ	57.47	35.53	73.37	51.93	66.71	62.95	81.35	78.92	77.83
ASP147@CG-HIS140@ND1.HD1	38.91	20.51	15.12	46.31	52.45	64.40	0.10	49.72	25.20
GLU152@CD-ARG148@CA.CZ	34.72	23.28	30.46	50.64	38.77	40.89	46.23	19.42	28.72
GLU152@CD-ARG151@CA.CZ	33.62	36.68	31.59	39.79	34.66	41.93	40.73	50.43	37.97
ASP144@CG-ARG148@CA.CZ	27.93	85.55	75.43	32.47	52.25	49.01	2.48	34.45	52.88
ASP147@CG-ARG151@CA.CZ	19.40	48.61	27.63	27.83	20.75	25.65	2.98	51.53	51.65
HIS187@NE2-ARG156@CA.CZ	14.09	59.43	68.19	64.04	18.17	53.34		21.77	14.53
HIS187@CG-ARG156@CA.CZ	0.04	0.13	0.33	5.29	0.35	11.79		1.03	4.23
GLU221@CD-ARG164@CA.CZ		38.33	6.32	0.02	0.25	0.33	0.48	0.33	0.07
ASP178@CG-HIS177@ND1.HD1	13.85	23.91	0.40	15.38	14.53	12.28	29.15	20.82	21.22
GLU211@CD-HIS177@ND1.HD1	8.29	4.67	88.56	23.20	24.23	7.75	24.53	8.77	7.85
GLU196@CD-ARG156@CA.CZ	5.51	10.04	16.45	65.75	0.86	42.63	0.05	28.88	36.37
GLU186@CD-HIS187@ND1.HD1	5.13	0.81	0.29	7.95	26.29	1.13	80.43	5.88	9.35
HIS187@CG-LYS185@CA.NZ	2.03	0.13	0.62	0.16	1.18	0.32	0.57	1.20	3.63
ASP202@CG-ARG156@CA.CZ	1.69	2.19	21.40	5.68	3.33	1.07	0.50	0.67	2.10
GLU207@CD-HIS177@ND1.HD1	0.77	1.70	6.87	6.35	5.36	1.39	6.30	1.32	1.58
ASP144@CG-HIS140@ND1.HD1	0.22	1.53		0.64	0.83	10.14	17.32	10.10	0.32
HIS155@NE2-ARG136@CA.CZ	0.18	3.15	0.15	0.53	0.19	0.61	3.63	3.53	0.12
HIS155@CG-ARG136@CA.CZ		0.29		0.05	0.01	0.07	0.50	0.88	
HIS140@NE2-ARG208@CA.CZ	0.17					0.03		4.02	19.77
HIS155@NE2-ARG151@CA.CZ	0.14	0.83	0.97		0.10	0.01	38.38*	20.33	32.00
HIS155@CG-ARG151@CA.CZ		0.04	0.01		0.01		49.22*	18.75	41.98
GLU196@CD-HIS155@ND1.HD1	0.06		0.51	11.34	0.17	6.62	0.05	2.35	4.05
GLU196@CD-HIS187@ND1.HD1		0.03	0.75	0.08	0.01	0.15	0.28	1.07	1.40
HIS187@NE2-HIS155@ND1.HD1	0.01		0.05	0.25	0.07	0.83	0.02	0.05	
GLU152@CD-HIS155@ND1.HD1	0.01	4.61		0.42	0.45	0.01	30.00*	35.52	30.53
GLU146@CD-LYS204@CA.NZ	0.01		2.18	0.57	0.02	0.01			
GLU200@CD-LYS204@CA.NZ		0.07			0.03	0.09	2.12	0.32	0.23
HIS155@NE2-LYS194@CA.NZ			0.88	3.34	2.05		0.03	1.63	0.23
GLU211@CD-HIS140@ND1.HD1				0.25		0.01		1.93	0.48
HIS140@NE2-ARG136@CA.CZ				0.17			5.18	4.73	5.00
HIS155@CG-LYS194@CA.NZ				0.16	0.17			0.33	
HIS140@NE2-ARG151@CA.CZ				0.15	0.01	0.03	5.60	1.52	8.05
HIS187@NE2-LYS194@CA.NZ				0.04			1.60	0.03	2.50
GLU146@CD-HIS140@ND1.HD1	0.06						1.93	2.92	22.98
ASP202@CG-LYS204@CA.NZ		0.01					1.68	0.02	

- ARG164-GLU221 - linking the  $\beta$ 2- $\alpha$ 2 loop and H3,
- GLU196-LYS194 - in the H2-H3 loop,
- GLU196-ARG156 - linking H1 and the loop of H2-H3,
- HIS187-ARG156 - linking H2 and the  $3_{10}$ -helix after H1,

and at 450 K, the SBs in H1 such as HIS155-ARG151, HIS155-GLU152 are having high occupied rates and seeing Table 2 we may know that there are many low occupied rate SBs not owned at 300 K and 350 K. The removal of all these SBs under low environment will lead to the changes of H1 and H2 region of BufPrP from  $\alpha$ -helices structures (BufPrP<sup>C</sup>) into  $\beta$ -sheet structures (BufPrP<sup>Sc</sup>). Our furthermore analyses of the B-factor and RMSF figures of [Zhang, 2018] can also give conformations of the findings from these SBs.

Table 2: Percentages (%) of some salt bridges (between two residues) under neutral pH environment for BufPrP at 300 K, 350 K and 450 K during 30 ns' MD (continuation):

Buffalo PrP/ Salt Bridges (SBs)	300 K			350 K			450 K		
	seed1	seed2	seed3	seed1	seed2	seed3	seed1	seed2	seed3
GLU146@CD-ARG151@CA.CZ							25.58	13.33	1.33
HIS140@CG-ARG151@CA.CZ							6.47	2.70	4.92
HIS140@CG-ARG148@CA.CZ							0.17	0.02	0.08
HIS140@NE2-ARG148@CA.CZ							1.18	0.03	0.22
HIS187@CG-LYS194@CA.NZ							1.52		0.32
GLU146@CD-ARG148@CA.CZ							16.88	3.52	
HIS140@CG-HIS155@ND1.HD1							8.57	0.02	1.85
HIS140@NE2-HIS155@ND1.HD1							5.82	0.02	1.93
HIS140@NE2-ARG156@CA.CZ							2.08		
HIS140@CG-ARG156@CA.CZ							1.25		
HIS155@CG-HIS140@ND1.HD1							8.03	0.02	1.93
HIS155@NE2-HIS140@ND1.HD1							7.78	0.03	2.47
ASP202@CG-LYS194@CA.NZ							6.57		
GLU152@CD-ARG156@CA.CZ							6.27	5.30	5.30
ASP147@CG-LYS194@CA.NZ							5.15		
ASP147@CG-LYS204@CA.NZ							1.80		
ASP147@CG-ARG208@CA.CZ								0.03	
GLU207@CD-LYS185@CA.NZ							3.48		0.02
GLU152@CD-HIS140@ND1.HD1							3.28		
GLU152@CD-ARG136@CA.CZ								0.18	
GLU152@CD-LYS194@CA.NZ							1.70		0.27
GLU221@CD-ARG136@CA.NZ							1.80		
GLU221@CD-ARG136@CA.CZ								0.85	
GLU221@CD-HIS140@ND1.HD1								11.73	
GLU200@CD-LYS185@CA.NZ							1.55		
GLU200@CD-HIS187@ND1.HD1							1.15		
HIS140@NE2-ARG220@CA.CZ							0.93		
HIS140@CG-ARG220@CA.CZ							0.63		
GLU186@CD-ARG156@CA.CZ							0.60		
ASP202@CG-ARG148@CA.CZ							0.42		
ASP144@CG-ARG208@CA.CZ							0.27		
ASP144@CG-ARG151@CA.CZ							0.23	1.83	
ASP144@CG-HIS155@ND1.HD1							0.18	0.25	
GLU200@CD-LYS194@CA.NZ							0.17		
ASP167@CG-ARG164@CA.CZ							0.15		
GLU196@CD-ARG148@CA.CZ							0.13		
GLU196@CD-HIS140@ND1.HD1							0.03		
GLU146@CD-HIS155@ND1.HD1							0.10	0.08	
ASP202@CG-HIS140@ND1.HD1							0.07		
HIS177@NE2-ARG208@CA.CZ							0.02		
HIS177@NE2-LYS185@CA.NZ							0.02		
HIS140@CG-ARG208@CA.CZ								2.85	6.77
ASP202@CG-HIS187@ND1.HD1								1.07	3.02
ASP147@CG-HIS155@ND1.HD1								0.02	0.02
ASP147@CG-ARG136@CA.CZ								0.22	
HIS187@NE2-LYS185@CA.NZ							1.05		
ASP144@CG-ARG136@CA.CZ								0.03	
HIS140@NE2-LYS204@CA.NZ									0.03
HIS155@NE2-ARG148@CA.CZ							0.02	0.05	
GLU196@CD-LYS185@CA.NZ							0.03		
GLU146@CD-ARG136@CA.CZ							0.05	6.10	
GLU146@CD-ARG208@CA.CZ								4.05	0.03
HIS155@CG-HIS187@ND1.HD1									0.02
HIS140@CG-ARG136@CA.CZ							2.45	3.90	1.45

## A concluding remark

This brief article talks about the MD results of BufPrP at different temperatures, and presents a clue (from the salt bridge point of view) to seek the reasons of the conversion from normal cellular prion protein (PrP<sup>C</sup>) to diseased infectious prions (PrP<sup>Sc</sup>). This should be very useful for the goals of medicinal chemistry in prion diseases research fields.



## References

Chen XL, Chen X, Liu YF (2016) Investigation on salt bridge interactions of mammalian prion proteins by molecular dynamics simulation. *Turkish J Biochem* 41(3):177-188.

Daude N (2004) Prion diseases and the spleen. *Viral Immunol* 17(3):334-349.

Griffith JS (1967) Self-replication and scrapie. *Nature* 215(5105):1043-1044.

Iannuzzi L, Palomba R, Di Meo GP, Perucatti A, Ferrara L (1998) Comparative FISH-mapping of the prion protein gene (PRNP) on cattle, river buffalo, sheep and goat chromosomes. *Cytogenet Cell Genet* 81(3-4):202-204.

Imran M, Mahmood S, Babar ME, Hussain R, Yousaf MZ, Abid NB, Lone KP (2012) PRNP gene variation in Pakistani cattle and buffaloes. *Gene* 505(1):180-185.

Jones CE, Klewpatinond M, Abdelraheim SR, Brown DR, Viles JH (2005) Probing  $\text{Cu}^{2+}$  binding to the prion protein using diamagnetic  $\text{Ni}^{2+}$  and  $^1\text{H}$  NMR: the unstructured N terminus facilitates the coordination of six  $\text{Cu}^{2+}$  ions at physiological concentrations. *J Mol Biol* 346(5):1393-1407.

Ogayar A, Snchez-Prez M (1998) Prions: an evolutionary perspective. *Int Microbiol* 1(3):183-190.

Oztabak K, Ozkan E, Soysal I, Paya I, Un C (2009) Detection of prion gene promoter and intron1 indel polymorphisms in Anatolian water buffalo (*Bubalus bubalis*). *J Anim Breed Genet* 126(6):463-467.

Pan KM, Baldwin M, Nguyen J (1993) Conversion of  $\alpha$ -helices into  $\beta$ -sheets features in the formation of the scrapie prion proteins. *Proc Natl Acad Sci U S A* 90(23):10962-10966.

Qing LL, Zhao H, Liu LL (2014) Progress on low susceptibility mechanisms of transmissible spongiform encephalopathies. *Dongwuxue Yanjiu* 35(5):436-445.

Reilly CE (2000) Nonpathogenic prion protein ( $\text{PrP}^C$ ) acts as a cell-surface signal transducer. *J Neurol* 247(10):819-820.

Uchida L, Heriyanto A, Thongchai C, Hanh TT, Horiuchi M, Ishihara K, Tamura Y, Muramatsu Y (2014) Genetic diversity in the prion protein gene (PRNP) of domestic cattle and water buffaloes in Vietnam, Indonesia and Thailand. *J Vet Med Sci* 76(7):1001-1008.

Yaman Y, Karadag O, n C (2017) Investigation of the prion protein gene (PRNP) polymorphisms in Anatolian, Murrah, and crossbred water buffaloes (*Bubalus bubalis*).

Trop Anim Health Prod 49(2):427–430.

Yaman Y, n C (2018) Nucleotide and octapeptide-repeat variations of the prion protein coding gene (PRNP) in Anatolian, Murrah, and crossbred water buffaloes. Trop Anim Health Prod 50(3):573–579.

Yu Z, Huang P, Yu Y, Zheng Z, Huang Z, Guo C, Lin D (2016) Unique properties of the rabbit prion protein oligomer. PLoS One 11(8):e0160874. doi: 10.1371/journal.pone.0160874.

Zhang JP (2010) Studies on the structural stability of rabbit prion protein probed by molecular dynamics simulations of its wild-type and mutants. J Theor Biol 264(1):119–122.

Zhang JP (2011) Comparison studies of the structural stability of rabbit prion protein with human and mouse prion proteins. J Theor Biol 269(1):88–95.

Zhang JP (2012) The nature of the infectious agents: PrP models of resistant species to prion diseases (dog, rabbit and horses). Prions and Prion Diseases: New Developments (J.M. Verdier Eds.), NOVA Science Publishers, ISBN 978–1–61942–768–6, Chapter 2, pp.41–48.

Zhang JP (2015) Molecular Structures and Structural Dynamics of Prion Proteins and Prions – Mechanism Underlying the Resistance to Prion Diseases, Springer, DOI: 10.1007/978–94–017–7318–8.

Zhang JP (2018) Molecular Dynamics Analyses of Prion Protein Structures – The Resistance to Prion Diseases Down Under, Springer, DOI: 10.1007/978–981–10–8815–5, Section 4.2, pages 87–92.

Zhang JP, Liu DDW (2011) Molecular dynamics studies on the structural stability of wild-type dog prion protein. J Biomol Struct Dyn 28(6):861–869.

Zhang JP, Wang F, Chatterjee S (2016) Molecular dynamics studies on buffalo prion protein. J Biomol Struct Dyn 34(4):762–777.

Zhang JP, Wang F, Zhang YL (2015) Molecular dynamics studies on the NMR structures of rabbit prion protein wild type and mutants: surface electrostatic charge distributions. J Biomol Struct Dyn 33(6):1326–1335.

Zhao H, Du Y, Chen S, Qing L, Wang X, Huang J, Wu D, Zhang Y (2015) The prion protein gene polymorphisms associated with bovine spongiform encephalopathy susceptibility differ significantly between cattle and buffalo. Infect Genet Evol 36:531–538. doi: 10.1016/j.meegid.2015.08.031.

Zhao H, Liu LL, Du SH, Wang SQ, Zhang YP (2012) Comparative analysis of the

Shadoo gene between cattle and buffalo reveals significant differences. PLoS ONE 7(10):e46601. doi: 10.1371/journal.pone.0046601.

Zhao H, Wang S, Guo L, Du Y, Liu L, Ma T, Otecko NO, Li C, Zhang Y (2017) Fixed differences in the 3'UTR of buffalo PRNP gene provide binding sites for miRNAs post-transcriptional regulation. *Oncotarget* 8(28):46006–46019.